VIBRATION INDUCED DROPLET GENERATION ON TEXTURED SURFACES

E. Y. Erdem[1], R. Baskaran[2,3], and K. F. Böhringer[2]
[1]Department of Mechanical Engineering, University of Washington, Seattle, WA, USA
[2]Department of Electrical Engineering, University of Washington, Seattle, WA, USA
[3]Components Research, Intel Corporation, Chandler, AZ, USA

ABSTRACT

We report a new method to create droplets from a large drop by using surface texture and vibration. Drops are vibrated on a PDMS substrate textured with ring shaped mesa structures. The vibrating contact line is modeled as a parametric oscillator. Droplets are created under the effect of pinning of the contact line, Laplace pressure difference on the mesa and inside the well and the spring force pulling the contact line back during vibration. We created droplets of 0.1-0.3μL from a 0.5mL drop by vibrating the drop at its third mode shape. Droplets are generated at the frequency of contact line oscillation of the drop.

1. INTRODUCTION

Droplet based microfluidic systems are becoming more popular due to their advantages over continuous-flow systems. Some of these advantages are ease of manipulation of various samples as individual packages [1], ability to achieve accurate volumes with precise concentrations, simpler fabrication and hence lower cost [2]. Droplet based microfluidic systems need to achieve four main tasks for completeness in droplet handling: generation, transportation, splitting and merging. Many platforms have been presented to manipulate droplets including electrowetting [3], thermocapillary actuation [4], and optical trapping [1].
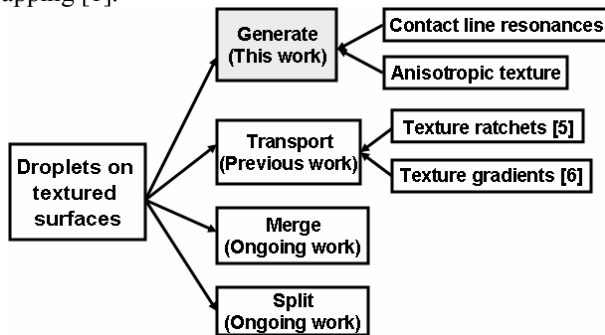

Figure 1: We propose a simple platform for droplet manipulation. Droplets can be generated, transported, merged and split by using surface texture. Previously the transport of droplets was achieved by using texture ratchets and gradients. In this paper we use vibration and surface texture to generate droplets from a large drop.

Our group previously presented methods for droplet transportation on texture-driven and vibration-actuated platforms [5, 6]. One advantage of these methods is that they do not involve any moving parts and hence have a simpler design and easy fabrication process. Here, we propose a novel method for droplet generation on the same platform (Figure 1).

2. VIBRATION OF DROPS

Vibration of large drops in gravity regime was studied in [7-9]. The substrate on which the drop stays is vibrated at various frequencies $f_E = \omega_E / 2\pi$ and accelerations $a(t) = -\omega_E^2 z \cos(\omega_E t) = -A\cos(\omega_E t)$, where z is the amplitude of the vertical displacement and A is the amplitude of acceleration of the substrate. There are two types of modes of vibration of a drop. By using the same terminology as in [7], *Type-I* modes keep a stationary (pinned) contact line whereas in *Type-II* modes the contact line oscillates. *Type-I* modes are observed below a threshold of amplitude of acceleration magnitude A_u. Above this threshold, the contact line overcomes hysteresis and starts to oscillate. Above a second threshold A_c the contour starts to fluctuate and eventually reaches a stable regime when it oscillates at $\omega_E / 2$ with large amplitudes and axisymmetric mode shapes. Mode 0 of *Type-II* is seen between the two thresholds while modes 2 and 3 are seen for accelerations above the second threshold.

The experimental set-up is composed of a high speed camera, a loudspeaker, an audio amplifier, a function generator and an oscilloscope. Figure 2 shows the top view of water drops in *Type-II* modes 0 and 3 on a smooth PDMS surface and a schematic of their side view.
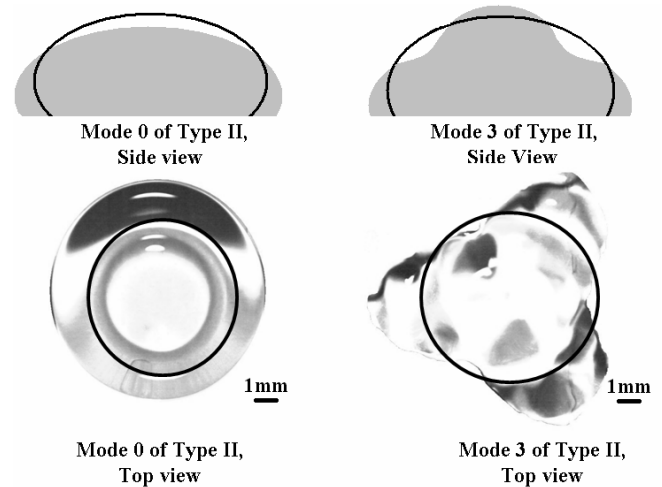

Figure 2: Drop vibration modes of Type-II. The volume is 0.5mL. The solid lines indicate the contour and contact line of the drop at rest, respectively.

To the first order, the contact line motion can be modeled as a parametric resonator [10]. The vibration of the contour around its equilibrium is described by Mathieu's equation [8] where the eigen frequency is a function of time:

$$\ddot{u} + \omega_m^2 \left(1 + h\cos\omega_E t\right)u = 0 \qquad (1)$$

where u is the deformation of contact line $(R(\varphi,t) = R_e + u(\varphi,t))$, ω_m is the resonant frequency of mode m, ω_E is the excitation frequency, R_e is the drop radius at equilibrium and $h = 3\Delta R/R$. For $\omega_E \ll \omega_0$, the fluctuations are quasistatic hence $h = 3\Delta R/R \cong 3A/4g$. The dispersion relation is given as follows [8, 9]:

$$\omega_m^2 = \Im m(m^2 - 1)/\rho e_c R_e^3 \qquad (2)$$

where $\Im$ is line tension $\left(\Im \approx \theta_e^2 \gamma \kappa^{-1}/2\right)$, e_c is the thickness of the drop $\left(e_c \approx \kappa^{-1}\theta_e\right)$, θ_e is the equilibrium contact angle on smooth PDMS surface and ρ is the density.
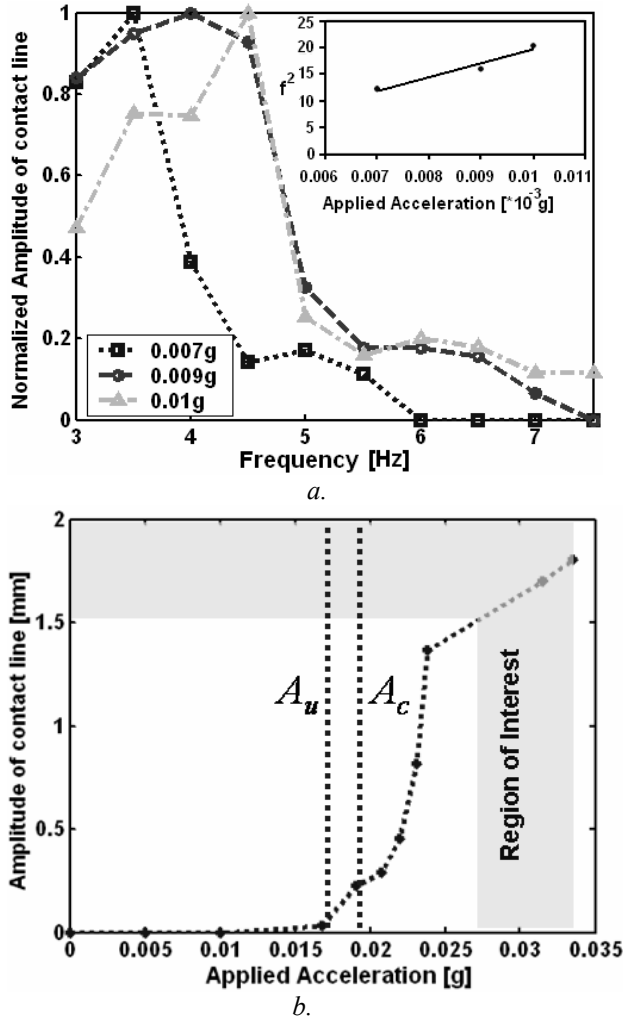

a.

b.

Figure 3: a) Normalized amplitude of contact line versus frequency at three different accelerations on smooth PDMS surface. The linear dependence of the squared excitation frequency on the applied acceleration results in parametric oscillations. The drop is 0.5mL. b) Amplitude of contact line oscillations versus acceleration at 6Hz. Below a threshold A_u, the contact line is pinned. Above the second threshold A_c, a small increase in acceleration causes a large change in the contact line amplitude, which is an indication of the parametric resonance. The drop is 0.5mL. The region of interest is the acceleration range, where we

obtain parametric resonance and hence the axisymmetric mode shapes.

Figure 3 shows the amplitude of contact line oscillations versus f_E $(f_E = \omega_E/2\pi)$ at various small accelerations applied to the system on smooth PDMS. For varying accelerations, the resonance frequency of contact line changes. The second plot shows the amplitude of contact line oscillation versus acceleration at $f_E = 6$ Hz. Below A_u the contact line remains pinned and above this threshold it starts to oscillate. Above A_c, a small change of acceleration causes a large change in the amplitude of oscillation as an indication of a parametric oscillator.

The threshold values of rough surfaces are different from the ones on smooth surfaces. The roughness of a surface is defined as follows:

$$r = \frac{total\ surface\ area}{total\ projected\ area} \qquad (3)$$

The Wenzel equation describes the effect of surface roughness on the contact angle of the drop [11]:

$$\cos\theta_w = r\cos\theta_e \qquad (4)$$

where θ_w is the contact angle on the rough surface. For a surface with $\theta_e > 90^o$ and $r > 1$ we have $\theta_w > \theta_e$. Hence the rough surface becomes more hydrophobic for hydrophobic surfaces. The contact angle on the smooth PDMS surface is measured as 113°, hence a roughness with $r > 1$ will increase this contact angle and will make the surface more hydrophobic. Figure 4 shows the amplitude of contact line oscillations versus acceleration at $f_E = 6$ Hz with $r = 1.16$. It is seen that the threshold values for rough surfaces are smaller than the values for smooth surfaces.
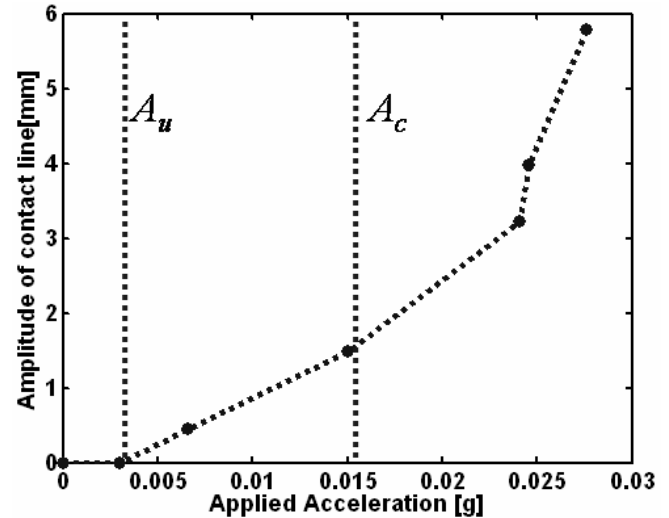

Figure 4: Amplitude of contact line versus applied acceleration at 6Hz on a PDMS surface with roughness 1.16. The drop that is vibrated is 0.5mL.

Figure 5 shows the amplitude of oscillation of different volumes (0.6mL<V<1mL) of drops at $f_E = 6$ Hz and

$A = 0.03$g on a smooth PDMS surface. The region of interest values for different volumes are different; however by looking at the graph below we can state that if we want to generate droplets 2mm away from the original position of the contact line we can use drops of volumes 0.4-0.8mL at 6Hz and $A = 0.03$g (shaded area in the graph).
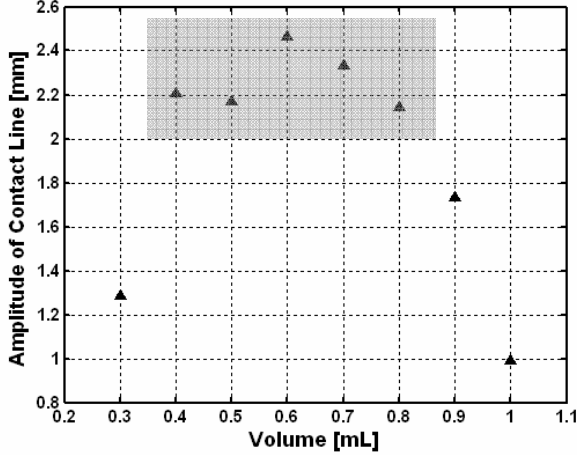
Figure 5: Amplitude of contact line oscillations versus volume of the drop at $f_E = 6$ Hz and acceleration amplitude of 0.03g on a smooth PDMS surface.

3. DROPLET CREATION

Design

In order to create droplets, we use surface texture to separate the edge of contact line in Type-II mode 3. The contact line is distorted by the surface texture and the distorted shape is unstable in terms of interfacial free energy.
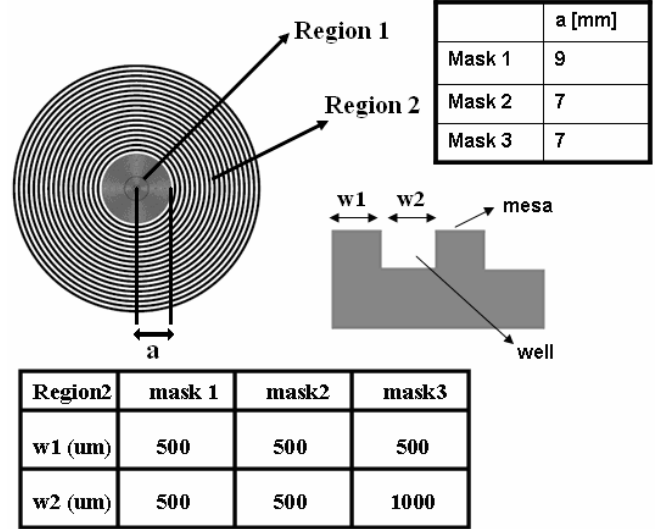
The substrates are fabricated in PDMS and the designs are composed of ring shaped mesa structures having ring shaped 'wells' (lower areas) in between (Figure 6). There are two regions in every design with different roughness. Region 1 is where the center of the drop is located and it has the same roughness for each design. When the drop vibrates, it expands on Region 2 which has a lower roughness –and hence is relatively less hydrophobic. This roughness change facilitates the motion of the contact line over Region 2.

Theory

Forces that affect the separation of droplets at the contact line are the restoring force due to vibration (spring force F_s), force arising from Laplace pressure difference between the mesa and wells, and the pinning. Here we neglect the dissipative forces (viscous dissipation and hysteresis).

The ring shaped structures form 'energy barriers' and the contact line gets pinned to a ring as it recedes back. The contact line also gets pinned during its outward motion; however this pinning is overcome for *Type-II* modes and does not affect the droplet formation.

The force caused by this pinning can be expressed as

Figure 6: Representative mask design for droplet creation. The parameters for 3 mask designs are given. The schematic on the right shows the cross section of the design and shows the 'mesa' and 'well'. 'w1' is the thickness of the ring shaped mesa and 'w2' is the width of the well. The drop is put on Region 1 where the surface area-air gap ratio is larger than other regions. When the drop vibrates, its contact line moves toward Region 2 and small droplets are created in that region.

$$F_p = L\gamma(1 - \cos\theta_e) \qquad (5)$$

where L is the length of the pinned contact line and γ is the surface tension between water and substrate.

The restoring force that pulls back the contact line can be derived from the equation of motion, (1), as

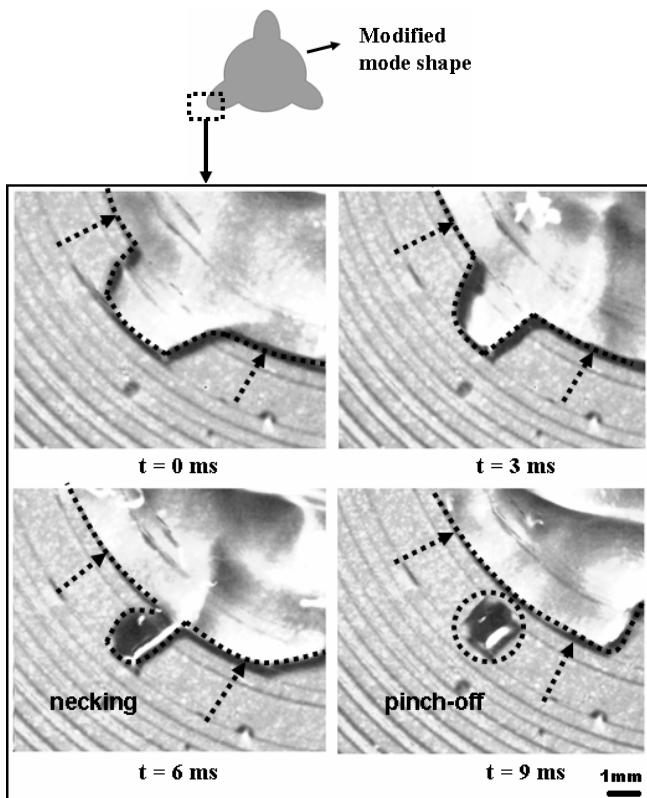$$F_s = m\omega_m^2(1 + h\cos\omega_E t)u \qquad (6)$$

Finally, the difference between the radii of curvature on the mesa and inside the well causes a pressure difference (Laplace pressure). The drop has two principle radii of curvature –in the plane parallel to the surface and in the plane perpendicular to the surface. The curvatures in the well and on the mesa are almost the same in the plane parallel to the surface. However in the plane perpendicular to the surface, the radius of curvature of the liquid inside the well ($R_{well}(t)$) is higher than the one on the mesa ($R_{mesa}(t)$). The corresponding force is given as follows:

$$F_L = A\gamma\left(\frac{1}{R_{mesa}(t)} - \frac{1}{R_{well}(t)}\right) \qquad (7)$$

This force pulls the water inside the well and causes shearing [12].

4. EXPERIMENTAL RESULTS

When vibrated at mode 3, the mode shape is modified due to the presence of rings (schematic in Figure 7). Under resonant frequencies, the contact line of the drop leaves droplets when receding. As shown in Figure 7, droplets of volumes as small as $0.1\,\mu L$ are created.

Figure 7: Snapshots of droplet generation at the contact line in mode 3. Laplace pressure on the mesa is higher than in the well, which causes shearing [12]. Distortion introduces instability and eventually a droplet is created inside the well. Tables show the average droplet volumes and number of droplets created for each mask for two different drop volumes.

f = 6Hz, Volume = 0.5mL

Mask	Volume of droplets [μL]	Number of droplets created
1	0.36	8
2	0.31	15
3	0.22	8

f = 6Hz, Volume = 0.7mL

Mask	Volume of droplets [μL]	Number of droplets created
1	0.16	5
2	0.2	15
3	0.1	9

5. CONCLUSION

In conclusion, we developed a novel method for droplet creation by using surface texture and vibration actuation. Droplets as small as 0.1μL are generated from a drop of 0.5mL. The method we used has global control variables (frequency and amplitude of acceleration) and surface texture. The method is implementable with low cost by PDMS molding.

We are currently working on integrated linear ratchet designs as in [5] in the radial direction for the transport of droplets after creation.

7. REFERENCES

[1] R. Mukhopadhyay, "Diving into Droplets", *Anal Chem*, vol. 78, pp. 1401-1404, 2006.

[2] S. Daniel, M.K.Chaudhury and P.-G. de Gennes, "Vibration-Actuated Drop Motion on Surfaces for Batch Microfluidic Processes", *Langmuir*, vol. 21, pp. 4240-4248, 2005.

[3] S.K. Cho, H. Moon, J. Fowler, C.J. Kim, "Splitting a Liquid Droplet for Electrowetting-Based Microfluidics", in *ASME IMECE*, New York, November 11-16, 2001.

[4] Y. Hennequin, D.G.A.L. Aarts, J.H. van der Wiel, G. Wegdam, J. Eggers, H.N.W. Lekkerkerker, D. Bonn, "Drop Formation by Thermal Fluctuations at the Ultralow Surface Tension", *Physical Review Letters*, vol. 97 (244502), 2006.

[5] A. Shastry, D. Taylor, K.F. Böhringer, "Micro-Structured Surface Ratchets for Droplet Transport" in *Transducers & Eurosensors Conference*, Lyon, France, June 10-14, 2007.

[6] A. Shastry, M.J. Case, K.F. Böhringer, "Directing Droplets Using Microstructured Surfaces", *Langmuir*, vol. 22, pp. 6161-6167, 2006.

[7] X. Noblin, A. Buguin, F. Brochard-Wyart, "Vibrated Sessile Drops: Transition between Pinned and Mobile Contact Line Oscillations", *The European Physical Journal E*, vol. 14, pp. 395-404, 2004.

[8] X. Noblin, A. Buguin, F. Brochard-Wyart, "Triplon Modes of Puddles", *Physical Review Letters*, vol. 94 (166102), pp. 1-4, 2005.

[9] X. Noblin, "Inertial Wetting and Dewetting: Triplons, Vibrated Puddles, Shock waves", PhD Thesis in *Physics*. 2004, University of Paris: Paris.

[10] V.I. Arnold, *Mathematical Methods of Classical Mechanics*. 2nd ed. Graduate Texts in Mathematics. 1989, New York: Springer.

[11] A. Shastry, M. Case, K.F. Böhringer, "Engineering Surface Texture to Manipulate Droplets in Microfluidic Systems", in *IEEE MEMS*, Miami Beach, FL, January 30- February 3, 2005.

[12] S. Sugiura, M. Nakajima, S. Iwamoto, M. Seki, "Interfacial Tension Driven Monodispersed Droplet Formation from Microfabricated Channel Array", *Langmuir*, vol. 17, pp. 5562-5566, 2001.